LA-UR- 09-04171

Approved for public release; distribution is unlimited.

Title: High Resolution Neutron Imaging of Water in the Polymer Electrolyte Fuel Cell Membrane

Author(s): Partha P. Mukherjee
Rangachary Mukundan
Jacob S. Spendelow
John R. Davey
Rodney L. Borup
Daniel S. Hussey
David L. Jacobson

Intended for: 216th ECS Meeting
Vienna, Austria
October 4-9, 2009

Los Alamos NATIONAL LABORATORY
EST. 1943

High Resolution Neutron Imaging of Water in the Polymer Electrolyte Fuel Cell Membrane

P. P. Mukherjee,[a] R. Mukundan,[a] J. S. Spendelow,[a] R. L. Borup,[a] D. S. Hussey,[b] D. L. Jacobson,[b] and M. Arif[b]

[a]Los Alamos National Laboratory, MS D429, MPA-11, Los Alamos, New Mexico, 87545, USA
[b]National Institute of Standards and Technology, Center for Neutron Research, 100 Bureau Drive, MS 8461, Gaithersburg, Maryland 20899, USA

Water transport in the ionomeric membrane, typically Nafion®, has profound influence on the performance of the polymer electrolyte fuel cell, in terms of internal resistance and overall water balance. In this work, high resolution neutron imaging of the Nafion® membrane is presented in order to measure water content and through-plane gradients *in situ* under disparate temperature and humidification conditions.

Introduction

Water uptake and transport characteristics in the polymer electrolyte fuel cell (PEFC) membrane are of paramount importance to the overall cell performance [1-4]. Water content in the ionomeric membrane, typically Nafion®, not only impacts the proton conductivity but also dictates the overall water balance in the fuel cell assembly. Water transport in the membrane is mainly governed by the electro-osmotic drag and back diffusion. Electro-osmotic drag causes transport of liquid water from anode to the cathode via proton mobility through the membrane, while back diffusion is responsible for water transport from the cathode to the anode side owing to a concentration gradient. The opposing transport modes determine the membrane hydration and the water gradient within the polymeric membrane, which further depend on the fuel cell operating conditions (e.g., current density, operating temperature, feed gas humidification). The effect of membrane water transport is typically accounted for by the net water transport coefficient from anode to cathode. While the net water transport coefficient is a generalized descriptor based on the overall cell performance, detailed characterization of the membrane water gradients is scarce.

The membrane water content and transport gradients are often inferred from the slope of the polarization curve and using ac impedance techniques [5,6], which warrant direct and *in situ* measurement of water profiles in the membrane for fundamental understanding. Bellows *et al.* [7] were the first to characterize water content and concentration gradients in a thick (500 μm) Nafion® membrane as a function of inlet relative humidity and applied current using low resolution neutron scattering at NIST (National Institute of Standards and Technology) Center for Neutron Research at Gaithersburg, Maryland, USA. Recent attempts to directly measure water content and distribution in the PEFC Nafion® membrane include magnetic resonance imaging by Tsushima *et al.* [8] and energy dispersive X-Ray scattering by Isopo and Albertini [9]. The primary advantage of neutron radiography over other techniques is the relatively low scattering cross-section of the various components used in the construction of a PEFC including Al, C, Pt, F and Si as compared to the scattering cross section of hydrogen present in liquid water [7,10]. This allows for the evaluation of the liquid water (vapor has 1000 times lower density and hence 1000 times lower neutron attenuation coefficient) content in unmodified commercial fuel cells since the neutrons easily penetrate them. In this work, we present high resolution neutron imaging of the PEFC Nafion® membrane and take a closer look into the membrane water uptake and transport characteristics.

Neutron Imaging

High resolution neutron imaging of bare Nafion® membranes as well as in membrane-electrode-assemblies (MEA) operated in both fuel cell and hydrogen pump modes were conducted at the NIST high resolution neutron imaging facility using the Microchannel Plate (MCP) detector with ~ 25 μm resolution and pixel pitch of ~ 15 μm [11]. The specific focus of this paper is on the evaluation of water content and through-plane gradients in the Nafion® membrane in a non-operating fuel cell. The cell assembly amenable to the Neutron beam experiment, shown in Fig. 1, has 2.25 cm^2 active area and 1 cm linear water imaging depth with metal hardware and does not contain hydrocarbon materials. The flow-field configuration consists of 9 parallel channels with 0.635 mm channel width each and 8 lands with 1.1 mm width each.

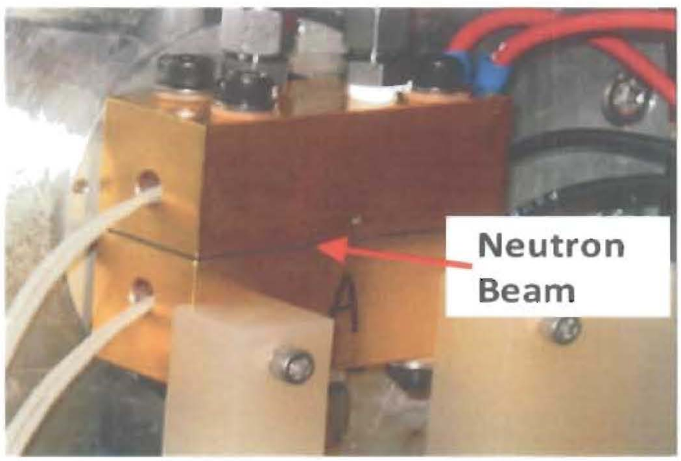

Figure 1: PEFC fixture for the Neutron Beam Experiment.

For neutron imaging in PEFCs, a dry cell is imaged first to provide a reference and the wet images are normalized with respect to this dry image. For example, the water thickness (t) image of a cell operated under any condition can be obtained by applying the Lambert-Beer law of attenuation by normalizing (dividing) the wet image intensity (I) by the dry image intensity (I_0) and using this intensity ratio to calculate water thickness from Eq. (1):

$$t = \frac{-1}{\mu_w} \ln\left(\frac{I}{I_0}\right) \tag{1}$$

where μ_w = water attenuation coefficient. Each detector system has to be calibrated using different known water thicknesses in order to obtain the attenuation coefficient for water. Moreover, the cell needs to be completely dry in order to avoid underestimating the water content. Moreover, due to thermal expansion of the various cell components, the dry image and the wet image must be obtained at the same temperature. The swelling/shrinking behavior of fuel cell materials (especially the proton exchange membrane) during the wetting and drying process has to be taken into account while analyzing the images. However this has not proven to be a problem for most of the fuel cell measurements where these materials are compressed between metal end plates. Generic details about neutron experiment, data treatment and quantification in the context of PEFC water measurement and visualization are furnished by Kramer *et al.* [12].

Results and Discussion

The first cell configuration consists of a single Nafion® 117 membrane sandwiched between the anode and cathode parallel channel flow-fields. High resolution neutron imaging was conducted with the cell placed vertically in the neutron beam in both vapor and liquid water equilibration modes. The effects of different humidification levels and equilibration temperatures on the membrane water content were investigated.

Figure 2 shows the neutron attenuation response in terms of water thickness in the vapor equilibrated Nafion® 117 membrane over time at 40^{0}C with 100% relative humidity (RH) in the anode and cathode flow-fields. Figure 3 exhibits the water thickness response in the liquid equilibrated membrane at 40^{0}C with liquid water feeds in both the anode and cathode channels. The vapor equilibrated mode shows significant instability with equilibration time, while the liquid equilibrated mode exhibits negligible variation with time. The vapor mode requires a longer time for the membrane to equilibrate. It is also important to note that there is a marked disparity in the water accumulation response between the two flow-fields in the liquid equilibrated mode. This difference could be attributed to the entrapment of air bubbles and water maldistribution among the channels.

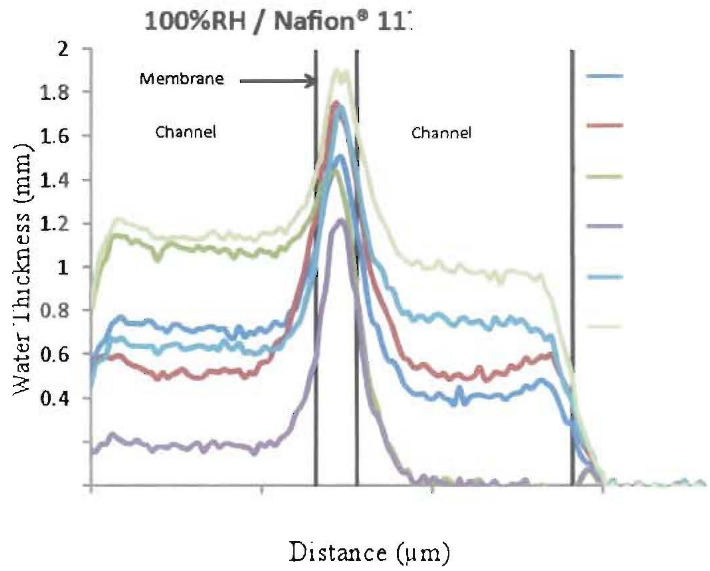

Figure 2: Vapor equilibration response with time for the single, bare Nafion® 117 membrane configuration.

Figure 4 shows the water content and gradient response in terms of water thickness for the single, bare Nafion® 117 membrane at 40^{0}C for varying anode/cathode RH combinations. As expected, with enhanced humidification level, the maximum water content in the membrane increases. The even anode/cathode humidification levels do not exhibit any perceivable gradient in the membrane. It is to be noted that the 25 μm resolution of the neutron detector precludes the possibility of a flat water content profile in the 175 μm thick Nafion® 117 membrane, which instead manifests as a peak toward the center of the membrane. The liquid/liquid equilibrated membrane shows a water gradient. This apparent gradient could be attributed to the air bubble formation in the channels leading to the lack of uniform filling with liquid water on the anode and cathode sides.

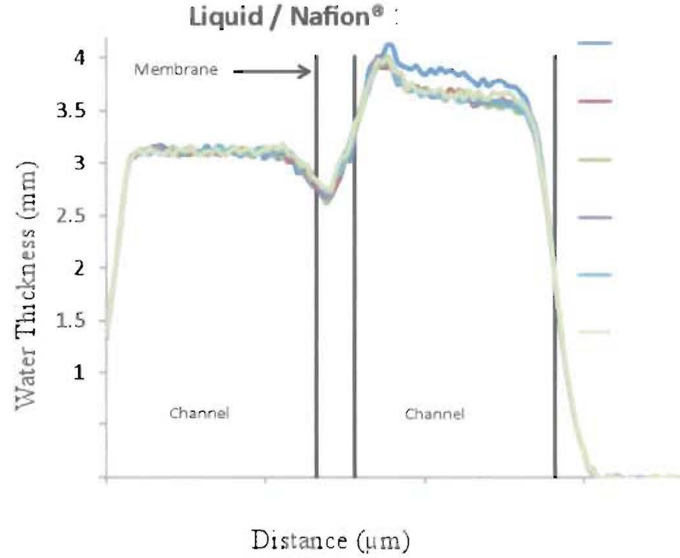

Figure 3: Liquid water equilibration response with time for the single, bare Nafion® 117 membrane configuration.

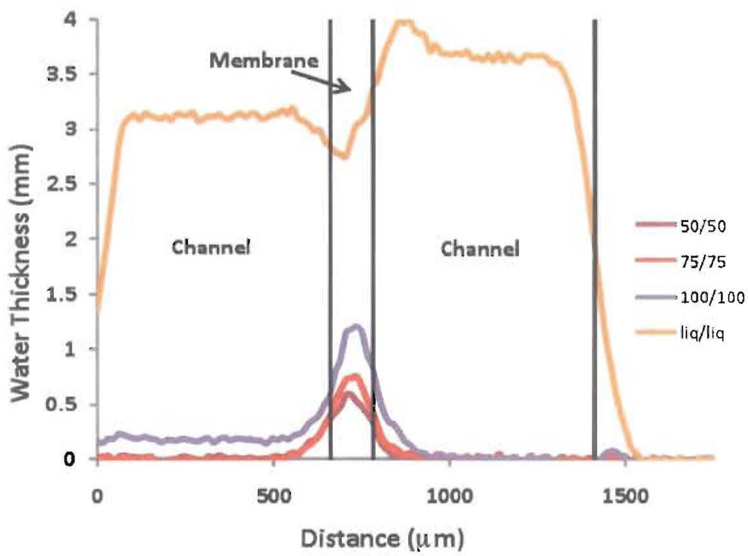

Figure 4: Water distribution for the single, bare Nafion® 117 membrane configuration at 40^0C in liquid equilibrated and vapor equilibrated modes under varying humidification levels.

Figure 5 shows the Nafion® 117 membrane water content and gradient response at 80^0C for varying anode/cathode RH combinations. The elevated temperature in general exhibits higher water uptake as compared to that at 40^0C and corroborates with the earlier observations [2,4]. The combination of 100% RH and liquid water in the flow-fields indeed displays a large water gradient in the membrane. Finally, the apparent water gradient in the membrane for the liquid/liquid case could be attributed to the disparity in the channel filling behavior owing to air bubble entrapment.

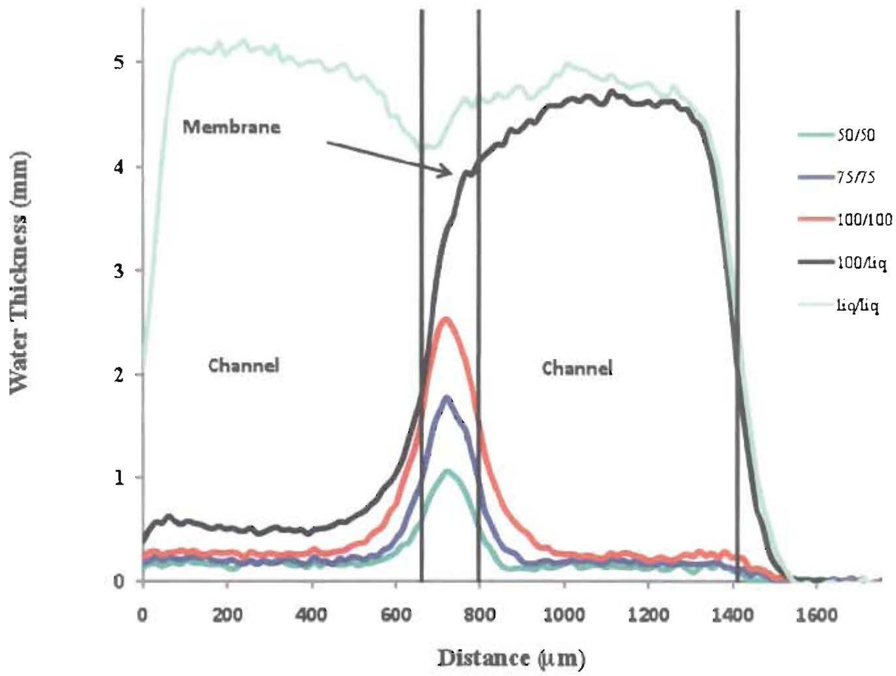

Figure 5: Water distribution for the single, bare Nafion® 117 membrane configuration at 80^0C in liquid and vapor equilibrated modes under varying humidification levels.

The membrane water content (λ), defined as the number of water molecules per SO_3^- acid group, were evaluated for both vapor and liquid equilibration from the neutron intensity data and is shown in Fig. 6 along with the results reported by Zawodzinski *et al.* [2] and Hinatsu *et al.* [4]. The measured water content values from the current neutron imaging study exhibit different response to vapor and liquid equilibration, thereby display Schroeder's paradox [13] and agree reasonably well with the reported data in the literature [2,4]. This study, however, does not make any specific assumptions about the reliance of the water content values on the membrane thermal history, as recently reported by Onishi *et al.* [14]. It is worth noting that the absolute water content values evaluated from the neutron scattering data might differ slightly based on the total optical density calculation procedure currently being worked on.

In order to garner enhanced understanding about the water distribution in the PEFC membrane and circumvent the present resolution constraint (~25 μm) of neutron imaging, another cell configuration was designed with three Nafion® 117 membranes sandwiched as part of a conventional MEA in a PEFC assembly. The cell was placed horizontally in the high resolution neutron beam and imaging was conducted to study the influence of varying combinations of anode/cathode humidification levels in vapor and liquid equilibration modes. The adjoining catalyst layer and gas diffusion layers do not allow the thick membrane to swell extensively under liquid equilibration.

Figure 7 shows the water distribution in the three-layer Nafion® 117 membrane assembly at 80^0C under disparate RH combinations in vapor and liquid equilibration modes. The distinct water gradient is observed for the dry and liquid wet channel conditions. The water distribution also displays the absence of a flat water profile in the membrane both in the liquid and vapor equilibration modes. The intermediate peaks in the 3-layer membrane assembly could be attributed to the interface effects between the membranes since the surface properties of Nafion® are more hydrophobic than the bulk.

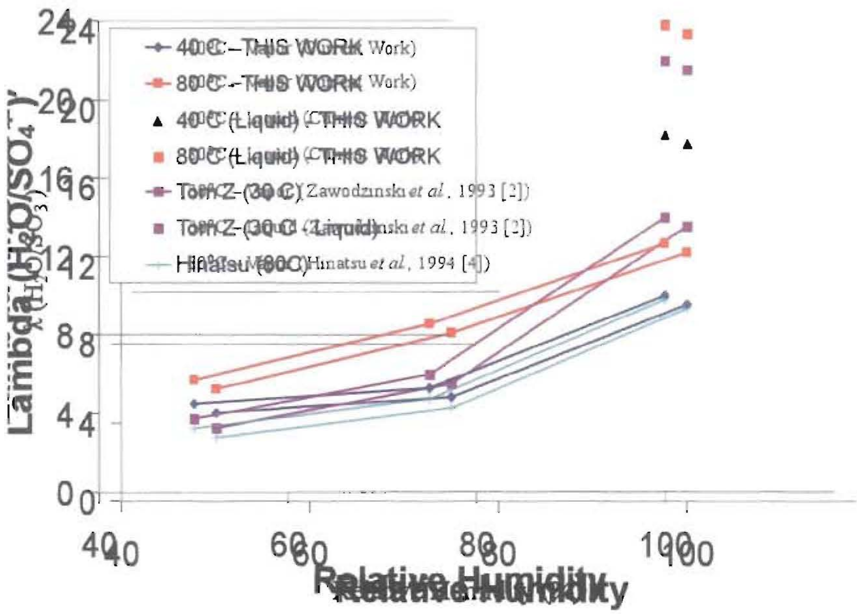

Figure 6: Water content estimates from the neutron scattering response for the single, bare Nafion® 117 membrane under vapor and liquid equilibrated conditions at two different temperatures along with reported values in the literature.

The average water content (λ) value corresponding to the liquid/liquid equilibration case was approximately calculated as 15.3, while the vapor/vapor equilibration case with 95% RH on both flow-fields gave rise to λ = 6. The water gradients with varying channel conditions from such experiment could be used to extract the back diffusion response of the membrane and correlated to fuel cell water balance.

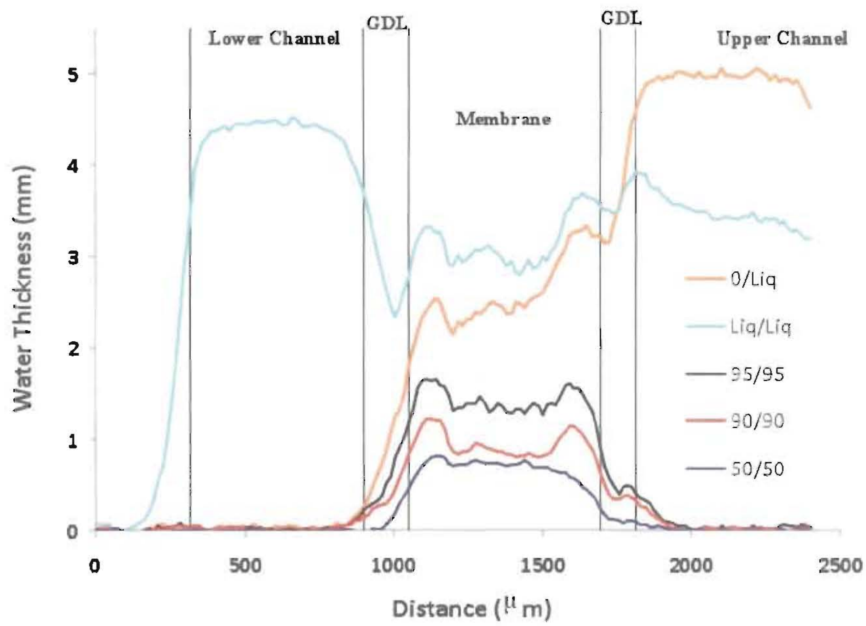

Figure 7: Water distribution for the 3-layer Nafion® 117 membrane in the MEA configuration at 80°C in liquid and vapor equilibrated modes under varying humidification levels.

In order to further understand the membrane response to water content and gradients, instead of a 3-layer membrane assembly, another configuration was specifically designed with a 40 mil (~1000 μm) thick Nafion® membrane from Ion Power. In one assembly, the 40 mil thick Nafion® membrane was sandwiched between two parallel flow-fields similar to the bare single Nafion® 117 configuration, described earlier. Another cell assembly was designed where the membrane was sandwiched as part of a MEA in a conventional PEFC assembly. The bare membrane-only configuration exhibited significant swelling and blocked the parallel channels on both sides in a liquid-equilibration mode experiment. The membrane in the MEA configuration was however sufficiently constrained by the adjoining catalyst layers and gas diffusion layers and extensive swelling was avoided. High resolution neutron imaging was conducted with the membrane in the MEA configuration in both fuel cell and hydrogen pump modes. Representative water thickness response from neutron scattering data with the membrane in the MEA configuration is shown in Fig. 8. The water distribution at the open circuit voltage (OCV) with 175% RH and 80^0C temperature shows a distinctive plateau and the average water content, λ, was approximately estimated as 18.7. Furthermore, the water gradient response from such hydrogen pump mode experiments could be used to extract the electro-osmotic drag response of the membrane and correlated to fuel cell water balance. Detailed analyses of the high resolution neutron imaging data for different cell configurations with bare membrane and under fuel cell and hydrogen pump modes are currently underway to develop a comprehensive understanding of the PEFC membrane water content and distribution.

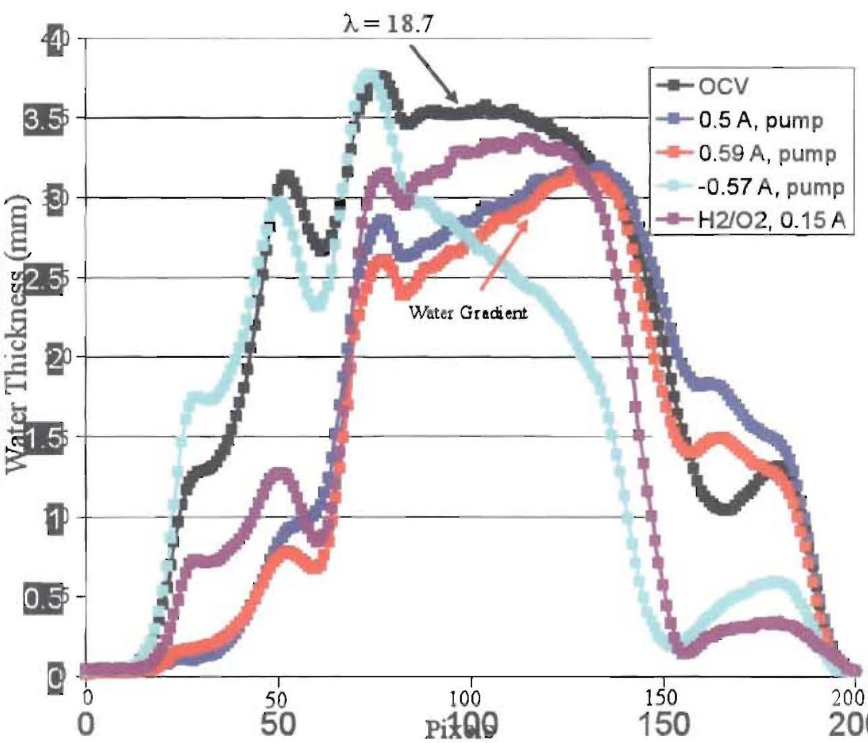

Figure 8: Water distribution for the 40 mil Nafion® membrane in the MEA configuration at 80^0C at OCV, hydrogen pump and operating fuel cell modes.

Conclusions

In this work, *in situ* measurements of water content and gradients in the PEFC Nafion® membrane are reported using high resolution neutron imaging for the first time. Different cell configurations with varying membrane combinations including a single Nafion® 117, a 3-layer Nafion® 117 assembly and a thick 40 mil Nafion® membrane were studied in vapor and liquid equilibrated conditions under bare membrane non-operating fuel cell, hydrogen pump and operating fuel cell modes. The water content values from the neutron imaging data for the single, bare Nafion® 117 membrane exhibit different response to vapor and liquid equilibration, and agree reasonably well with the reported data in the literature. The three-layer Nafion® 117 membrane assembly shows inter-membrane interfacial peaks in the water distribution response. The single layer 40 mil membrane, however, displays a distinct water content plateau at OCV. This high resolution neutron imaging study of the PEFC membrane is envisioned to provide a comprehensive understanding of the membrane water content, diffusion gradient and electro-osmosis response under disparate operating and materials combinations.

Acknowledgments

This work was supported by US Department of Energy, Office of Hydrogen, Fuel Cells and Infrastructure and Los Alamos National Laboratory LDRD Office. The supply of the 40 mil Nafion® membrane by Steve Grot at Ion Power is gratefully acknowledged.

References

1. T. E. Springer, T. A. Zawodzinski, and S. Gottesfeld, *J. Electrochem. Soc.*, **138**, 2334 (1991).
2. T. A. Zawodzinski, C. Derouin, S. Radzinski, R. J. Sherman, V. T. Smith, T. E. Springer, and S. Gottesfeld, *J. Electrochem. Soc.*, **140**, 1041 (1993).
3. T. A. Zawodzinski, T. E. Springer, J. Davey, R. Jestel, C. Lopez, J. Valerio, and S. Gottesfeld, *J. Electrochem. Soc.*, **140**, 1981 (1993).
4. J. T. Hinatsu, M. Mizuhata, and H. Takenaka, *J. Electrochem. Soc.*, **141**, 1493 (1994).
5. T. E. Springer, T. A. Zawodzinski, M. S. Wilson, and S. Gottesfeld, *J. Electrochem. Soc.*, **143**, 587 (1996).
6. F. N. Buchi and G. G. Scherer, *J. Electroanal. Chem.*, **404**, 37 (1996).
7. R. J. Bellows, M. Y. Lin, M. Arif, A. K. Thompson, and D. Jacobson, *J. Electrochem. Soc.*, **146**, 1099 (1999).
8. S. Tsushima, K. Teranishi, and S. Hirai, *Electrochem. Solid State Lett.*, **7**, A269 (2004).
9. A. Isopo and V. R. Albertini, *J. Power Sources*, **184**, 23 (2008).
10. R. Mukundan and R. L. Borup, *Fuel Cells*, in press (2009).
11. O. H.W. Siegmund, J. V. Vallerga, A. Martin, B. Feller, M. Arif, D. S. Hussey, and D. L. Jacobson, *Nuclear Instruments and Methods in Physics Research A*, **579**, 188 (2007).
12. D. Kramer, J. Zhang, R. Shimoi, E. Lehmann, A. Wokaun, K. Shinohara, G. G. Scherer, *Electrochimica Acta*, **50**, 2603 (2005).
13. P. Z. Schroeder, *Phys. Chem.*, **45**, 75 (1903).
14. L. M. Onishi, J. M. Prausnitz, and J. Newman, *J. Phys. Chem. B*, **111**, 10166 (2007).